Comparative Study of Irradiated and Non-Irradiated Recycled Polypropylene/Peanut Shell Powder Composites under the Effects of Natural Weathering Degradation

Nor Fasihah Zaaba and Hanafi Ismail *

The properties of irradiated and non-irradiated recycled polypropylene (RPP)/peanut shell powder (PSP) composites were investigated relative to the effects of 6 months exposure to natural weathering. RPP/PSP composites were prepared by melt-mixing and compression molding with 0 to 40 wt.% PSP loading. The fabricated composites were then irradiated using a 2.0 MeV electron beam accelerator at a fixed dose of 20 kGy. The properties of non-irradiated and irradiated composites after exposure to natural weathering were compared and characterized by tensile properties, scanning electron microscopy (SEM), carbonyl indices (CI), differential scanning calorimetry (DSC), and weight loss analysis. The results in tensile strength and tensile modulus of irradiated RPP/PSP composites increased, while elongation at break decreased. The thermal stability of irradiated composites was also improved compared with non-irradiated composites. Pores and fungus penetration were observed from the SEM morphology, while an increase in carbonyl index and weight loss of both composites were evidenced that degradation occurred. The overall results indicated that the irradiated RPP/PSP composites were more resistant to natural weathering degradation than the non-irradiated RPP/PSP composites.

Keywords: Electron beam irradiation; Recycled polypropylene; Peanut shell powder

*Contact information: School of Materials and Mineral Resources Engineering, USM Engineering Campus, Nibong Tebal, Penang, Malaysia; *Corresponding author: ihanafi@usm.my*

INTRODUCTION

Radiation technology is an alternative procedure of chemical modification in the development of new thermoplastic/natural filler composites. It is a process that can alter the chemical composition, structure, mechanical properties, and thermal properties of the polymeric materials (Albano *et al.* 2001). Crosslinking and degradation are the main effects induced in polymers by the ionizing radiation (Czvikovszky 1996; Khan *et al.* 1999; Alessi *et al.* 2007; Choi *et al.* 2008). Once the crosslinking becomes predominant, three-dimensional networks are formed. The process takes place by the recombination of radicals generated by irradiation of the polymer. In the course of crosslinking, the polymeric chains attach themselves *via* covalent joining generated by radiation. Thus, there can be a rise in the mechanical resistance, molecular weight, three-dimensional networks, and viscosity of the polymer while a reduction on the solubility as well as changes in the glass transition temperature in amorphous phase of the polymer. The end properties of the materials are strongly dependent on the degree of crosslinking. The crosslinked structure decreases the interfacial tension and improves the material properties (Zhai *et al.* 2003). However, the

irradiation dosage must be optimized to avoid unnecessary crosslinking, which can make the material brittle (Ismail *et al.* 2010; Bee *et al.* 2012; Nordin and Ismail 2013). According to Ishak Ahmad *et al.* (2012), the effective radiation dosage is in the range 20 to 30 kGy. Within this range, the EB irradiated composites show enhancement in the tensile strength and impact strength, indicating a higher interfacial bond strength and adhesion between the filler and the matrix. Besides, this mechanism also depends on the process conditions such as the presence of oxygen, type of radiation, additives, solvents, and degree of crystallinity.

In addition, there are few types of radiation sources such as x-ray, gamma (Cobalt-60 and caesium-137), and electron beam radiation. Since the 1970s, x-ray and gamma ray radiation have been investigated as one of the chemical modification methods for the development of polymer composites' properties. It has been evidenced to be a potential manufacturing process, particularly for thick polymer composites (up to 300 mm) due to the extra-high electromagnetic energy (Berejka *et al.* 2005; Dispenza *et al.* 2008). Nevertheless, the radiation time of x-rays and gamma is longer compared to electron beams due to the lower dose rates. Above all, x-ray and gamma radiation procedures comprise a critical potential hazard by employing high levels of radioactivity and producing hazardous, hardly disposable matter, such that it is not convenient to apply such methods in the composites industries (Youssef *et al.* 2009). Presently, the electron beam (EB) radiation technology is being substituted over other radiation sources due to their superficial advantages such as an effective large-scale processing, less time consumption, low cost, consistent sterilization, ease of operation, rapid improvement of properties, ability to irradiate of a variety of physical shapes, and there being no serious environmental threats (Sam *et al.* 2012a; Mizera *et al.* 2012; Aji *et al.* 2013). Indeed, EB radiation is able to modify the properties of the polymers comparable to x-ray and gamma radiations (Balaji *et al.* 2017).

Peanut shells are abundant agro-industrial waste products that are intractable to degradation under natural conditions (Zheng *et al.* 2013). The increasing growth of peanut production has led to the accretion of huge amounts of these shells all over the world. Peanut shells are renewable resources that could be targeted for purposeful use in the food, feed, bioenergy, and paper industries (Wilson *et al.* 2006). Much like other agricultural lignocellulosic biomass, peanut shells are composed mainly of cellulose (35.7%), hemicelluloses (18.7%), lignin (30.2%), protein (8.2%), carbohydrate (2.5%), and ash content (4.7%) (Raju *et al.* 2012). Lignin, a complex polymer, is the most recalcitrant component of plant biomass (Cesarino *et al.* 2012); it binds tightly to, and provides a physical seal around, cellulose and hemicellulose. The high lignin content of peanut shells is largely responsible for the resistance to biodegradation under normal environmental conditions (Fang *et al.* 2014). Hence, the use of peanut shells as natural fillers in thermoplastic/natural filler composites presents a new application path in the transformation of agro wastes to beneficial resources in plastic industries (Obasi, 2015).

In this study, recycled polypropylene (RPP) was used as a raw material for the continuous life cycle of a new product and sustainable manufacturing. Polypropylene (PP) is widely used as a polymer matrix material due to the fact that it has several outstanding properties for composite production. PP is very suitable for blending, reinforcing, and filling. PP with natural fibrous polymers is a natural-synthetic polymer composite (Shubhra *et al.* 2011; Chattopadhyay *et al.* 2010). Due to the recycling of PP, the lifetime of this plastic is prolonged, leading to the reduction of waste and use of non-renewable resources (Corbiere-Nicollier *et al.* 2001; Santiagoo *et al.* 2016).

To date, there has been no attempt to study the effect of EB irradiation on the

physical, thermal, mechanical, and morphological properties of recycled polypropylene (RPP)/peanut shell powder (PSP) composites after 6 months exposure to natural weathering. In this study, PSP was compounded with recycled polypropylene (RPP), and electron beam irradiation was used to enhance the interfacial adhesion between natural fillers and polymer matrix. The non-irradiated and irradiated RPP/PSP composites were exposed to natural weathering in Penang, Malaysia for 6 months. The degradation of both composites was compared by analyses of tensile properties, morphology, carbonyl indices, differential scanning calorimetry (DSC), and weight loss. It was expected that EB irradiation formed a crosslinking network that would enhance the properties of the irradiated RPP/PSP composites.

EXPERIMENTAL

Materials

Recycled polypropylene (RPP), with a melt flow index of 3 g/min, and peanut shell powder (PSP) were obtained from Zarm Scientific (M) Sdn. Bhd., Penang, Malaysia. The peanut shells were ground to particles in the size range of 70 to 250 μm. The PSP was dried for 3 h at 70 °C in a vacuum oven before the subsequent composite fabrication.

Composite Preparation and Processing

The PSP was compounded with RPP using an internal mixer (Haake Rheomix Mixer, Model R600/610, Karlsruhe, Germany) at 180 °C and 50 rpm to obtain a homogeneous sample. The RPP was charged into the mixer and melted for 4 min before the PSP was added. The compound was mixed for another 6 min to obtain the stabilization torque. The total mixing time was 10 min for all samples. The processed samples were compression-molded into a 1 mm-thick sheet in a heated hydraulic press (Kao Tieh Go Tech Compression Machine, Taichung, Taiwan) at 180 °C. Table 1 shows the formulation of the RPP/PSP composites.

Table 1. Formulation Characteristics of RPP/PSP Composites

Composite	RPP (wt.%)	PSP (wt.%)
RPP	100	-
RPP/10% PSP	90	10
RPP/20% PSP	80	20
RPP/30% PSP	70	30
RPP/40% PSP	60	40

Electron Beam Irradiation

The compression-molded samples were irradiated with an electron beam. The electron beam (EB) irradiation was conducted in Malaysia Nuclear Agency with an electron beam accelerator (model NHV EPS 3000, Nissin High Voltage, Kyoto, Japan). The thin sheet of the RPP/PSP composites was irradiated at ambient temperature using the following parameters: accelerating voltage, 1.5 MeV; beam current, 10 mA; dose per pass, 10 kGy; and absorbed dose, 20 kGy. Figure 1 shows the schematic diagram of electron beam accelerators irradiating composite samples.

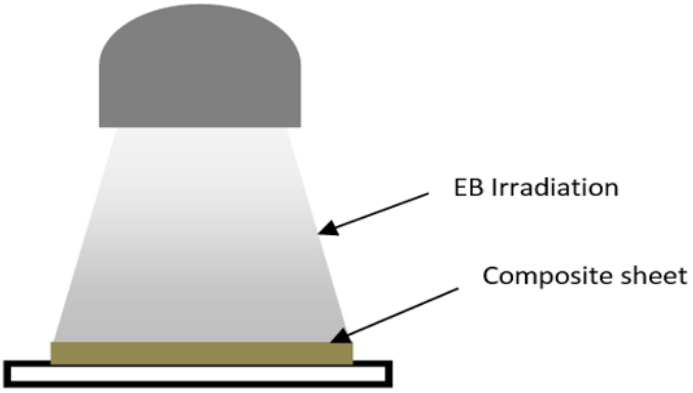

Fig. 1. Schematic diagram of electron beam accelerators irradiating composite samples

Outdoor Weathering Test

Outdoor weathering tests were operated for a duration of 6 months, from June to December 2016 at Universiti Sains Malaysia (latitude 5° 8' N, longitude 100° 29' E). The tests were conducted by subjecting the dumbbell-shaped samples of irradiated and non-irradiated composites to sunlight. The cumulative rainfall, average temperature, and relative humidity were taken from the closest meteorological station in Butterworth, Penang, Malaysia (latitude 5° 28' N, longitude 100° 23' E). The average of the data taken for each month is shown in Figs. 2 and 3. The tests were performed according to ISO 877.2 (2009). An exposure rack has been used to place the dumbbell-shaped samples of the composites by facing to the south and at an inclination angle of 45°. The samples were subjected to analytical and mechanical tests after 6 months of exposure. The samples were washed with distilled water and oven-dried at 70 °C to a constant weight.

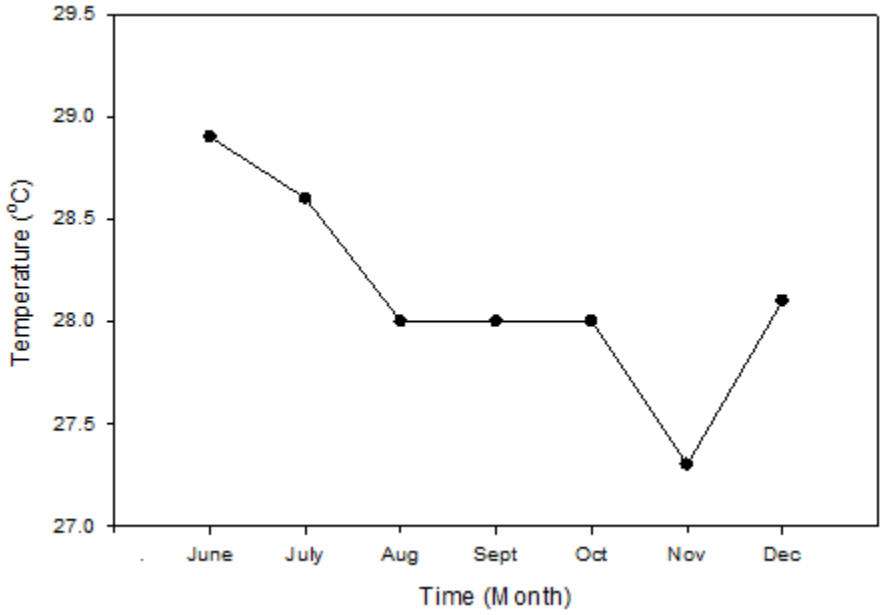

Fig. 2. Average temperature during outdoor natural weathering test from June to December 2016

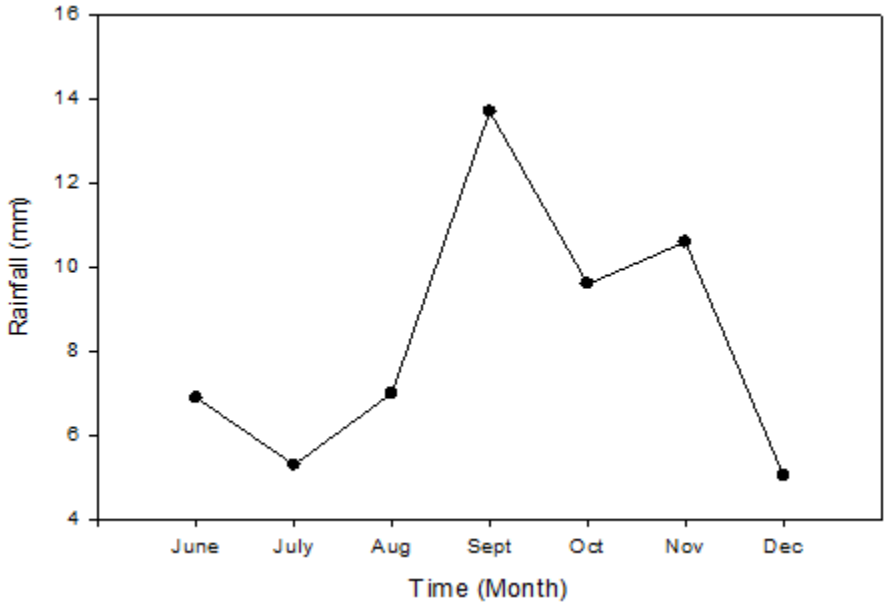

Fig. 3. Average per day of rainfall during outdoor natural weathering test from June to December 2016

Gel Content Analysis

The gel content of EB irradiated samples was determined using the solvent extraction method. The samples were positioned in folded 120-mesh stainless steel cloth cages. The samples and cages were weighed before and after extraction. The samples were refluxed with hot xylene for 24 h using a Soxhlet apparatus. The remaining insoluble sample was dried in a vacuum oven to a constant weight. Gel content was calculated as shown in Eq. 1.

$$\text{Gel content } (\%) = \frac{W_g}{W_o} \text{ X } 100 \quad (1)$$

where W_o is weight before the extraction and W_g is weight after the extraction.

Tensile Properties

Tensile strength, elongation at break, and tensile modulus of degraded samples were obtained from the tensile tests using a universal testing machine (model 3366, Instron, Canton, MA, USA) according to ASTM D638 (2014). Equation 2 shows the calculation of retention of these properties.

$$\text{Retention } (\%) = \frac{\text{Value after degradation}}{\text{Value before degradation}} \text{ x } 100\% \quad (2)$$

Surface Morphology

The surface changes of degraded samples were evaluated by scanning electron microscopy (SEM; model VPSEM SUPRA 35VP, Carl Zeiss Microscopy, Oberkochen, Germany). Before scanning the fractured surface, samples were sputter-coated with gold to avoid electrostatic charging. For degraded samples, 10 kV voltage was used to achieve deeper electron penetration.

Carbonyl Indices

Carbonyl index (CI) was used to estimate the degree of degradation of RPP/PSP composites. It was calculated from FTIR spectra, according to the baseline method, *i.e.*, the ratio of absorption bands at 1720 and 2910 cm^{-1}.

Differential Scanning Calorimetry

Differential scanning calorimetry measurements were performed in a Perkin Elmer DSC (DSC 6, Waltham, MA, USA). Approximately 4 mg of the composite sample was heated from room temperature to 200 °C at 10 °C/min and held for 5 min to eliminate the thermal history. The sample was cooled to room temperature and then reheated to 200 °C at 10 °C/min to trace the heating behavior. Each run was performed under a nitrogen atmosphere. From the maximum peak of DSC results, the melting temperature (T_m) and crystallization temperature (T_c) were obtained, while the area under the peak showed the heat of fusion (ΔH_f) of the RPP/PSP composites. Equation 3 shows the calculation of crystallinity of the RPP phase,

$$Xc\ (\%) = \frac{\Delta H_f}{(1-ww)\ X\ \Delta H_{100\%}} \times 100\ \% \quad (3)$$

where ΔH_f is the heat of fusion of the sample analyzed, ww is the filler fraction, and $\Delta H_{100\%}$ is the heat of fusion for 100% crystalline PP (207 Jg^{-1}) (Gupta *et al.* 2009).

Weight Loss

The weight loss of degraded samples was calculated according to Eq. 4,

$$\text{Weight loss}\ (\%) = \frac{(W_i - W_f)}{W_i} \times 100\% \quad (4)$$

where W_i is weight before degradation and W_f is weight after degradation.

RESULTS AND DISCUSSION

Gel Content Analysis

Figure 4 depicts the percentage of gel content of irradiated composites at different PSP loading after exposure to 6 months natural weathering. Generally, the formation of crosslinking in the composites system could be induced by the electron beam irradiation process. The percentage of extracted gel indicates the crosslink density of polymers (Ali *et al.* 2008; Murray *et al.* 2013). The irradiated RPP/PSP composites demonstrated a decrease in percentage of gel content following the addition of PSP loading (Fig. 4). It was found that, as PSP loading increased, the RPP loading was decreased. Thus, the formation of structural networks especially in RPP component became less prominent during the irradiation process. At lower PSP loading, the higher percentage of gel content indicated that more crosslinking reaction took place in the RPP component. The molecular structure of linear PP can be significantly modified by electron beam irradiation. Thus, the main reactions such as chain scission, chain branching, and crosslinking occurred during the irradiation process. Typically, all these reactions can happen simultaneously. For PSP, the mixture consisted of cellulose (35.7%), hemicelluloses (18.7%), lignin (30.2%), protein (8.2%), carbohydrate (2.5%), and ash content (4.7%). Chemically, irradiation causes cellulose depolymerization. However, it is difficult to selectively oxidize the cellulose

backbone (Henniges *et al*. 2013). Therefore, a radical reaction occurred with a higher amount of radicals in the polymer matrix and slightly in the natural fillers.

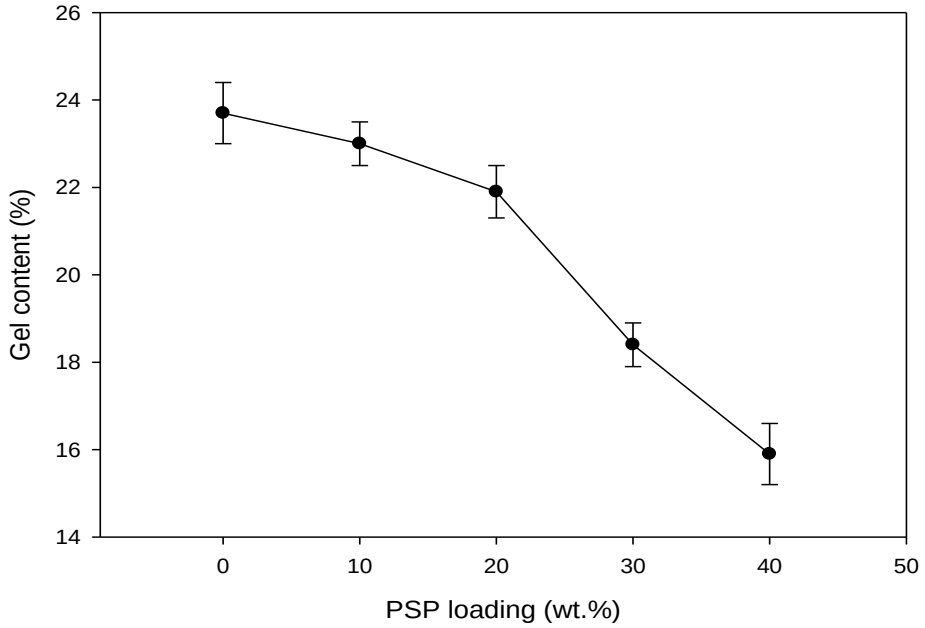

Fig. 4. Gel content of irradiated RPP/PSP composites at different PSP loading after 6 months natural weathering

Tensile Properties

Figure 5 shows the tensile strength of non-irradiated and irradiated RPP/PSP composites after 6 months exposure to natural weathering. As expected, the tensile strength for both composites decreased as PSP loading increased.

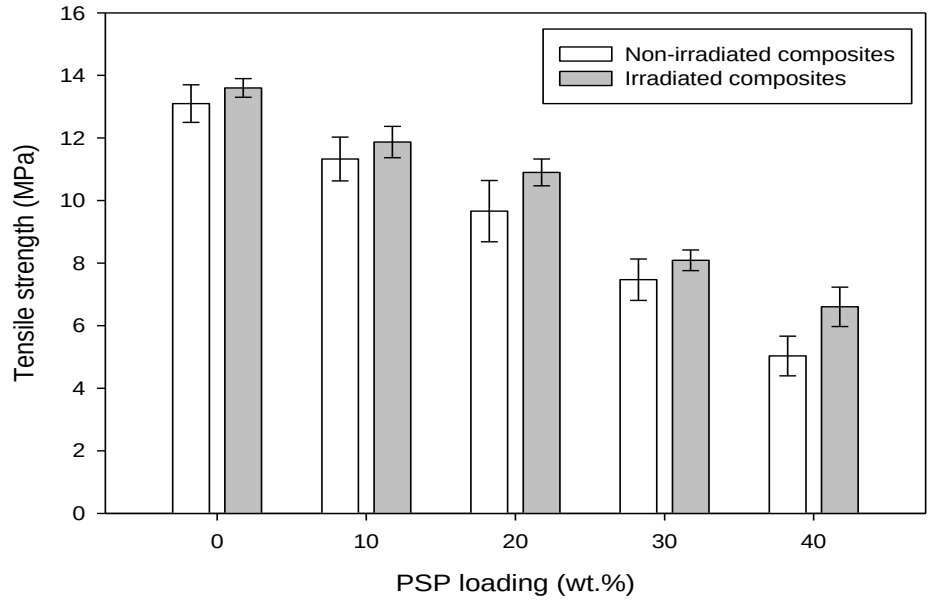

Fig. 5. Comparison of tensile strength after 6 months natural weathering

Similar results are shown in Table 2. Based on the retention values, the addition of PSP increased the degradability of the composites. This effect was due to the hydrophilic nature of PSP, which allows it to easily leach out upon exposure. The leaching effect generated crazes and pores on composite surfaces; subsequently, the RPP matrix was easily attacked by microorganisms, heat, and UV. The retention of tensile properties of irradiated composites was higher than non-irradiated composites, reflecting the difficulty in breaking the crosslinked structure (Fig. 8) of irradiated composites by degradation factors such as UV and heat. Ishak Ahmad *et al.* (2012) reported similar results in their study on the effect of EB irradiation on rice husk/natural rubber/high density polyethylene (RH/NR/HDPE) composites, whereas the radiation could have induced the crosslinking and chain scission in plastic phases as well as at the interface. This reduced the filler-matrix surface tension and improve the adhesion of the filler particles to the matrix. Evidence of the PSP filler embedded in RPP matrix can be observed in Fig. 10(a). Notably, irradiated composites can have greater antibacterial properties than non-irradiated composites (Zhai *et al.* 2003). In sum, the degradability of irradiated composites was lower than non-irradiated composites.

Table 2. Retention of Tensile Properties for Non-Irradiated and Irradiated RPP/PSP Composites after 6 Months Weathering

Sample	Retention of Non-irradiated Composites (%)			Retention of Irradiated Composites (%)		
	Tensile strength	Elongation at break	Tensile modulus	Tensile strength	Elongation at break	Tensile modulus
RPP	53.04	34.32	176.45	-	-	-
RPP/10% PSP	48.72	21.39	217.51	62.77	19.08	130.17
RPP/20% PSP	35.12	12.11	228.72	50.90	10.79	135.62
RPP/30% PSP	29.08	8.65	244.11	37.97	6.66	140.86
RPP/40%PSP	10.56	4.33	250.08	29.00	2.76	144.14

Figure 6 demonstrates the elongation at break of non-irradiated and irradiated composites after 6 months exposure to natural weathering. The trend of elongation at break was similar to that of tensile strength. The property of elongation at break is essential when seeking evidence of chain scission of polymer composites throughout degradation. The abiotic effects such as temperature, sunlight, wind patterns, and precipitation might cause chain scission (Gad 2009; Sabet *et al.* 2012; Sam *et al.* 2012b), which decreases the elongation at break of the exposed composites. The elongation at break of irradiated composites was lower than that of non-irradiated composites, as shown in Table 2. This was due to the crosslinked structures that were induced by irradiation, which locked the polymer chains and resisted the mobility of the polymer molecules. Hence, the capability of stretch deformation was reduced, resulting in lower elongation at break. Likewise, the decrement of elongation at break was also caused by the increment of PSP loading and the crystallinity of composites. As demonstrated by the DSC results in Table 3, the crystallinity of composites increased as PSP loading increased. Crystallinity refers to the degree of structural order in a solid or rigid segments. Thus, as crystallinity increases, the elongation at break is decreased due to the high rigid PSP segments over the flexible RPP segments. Similar findings were also reported by Salmah *et al.* (2011) for properties of low-density polyethylene/palm kernel shell composites.

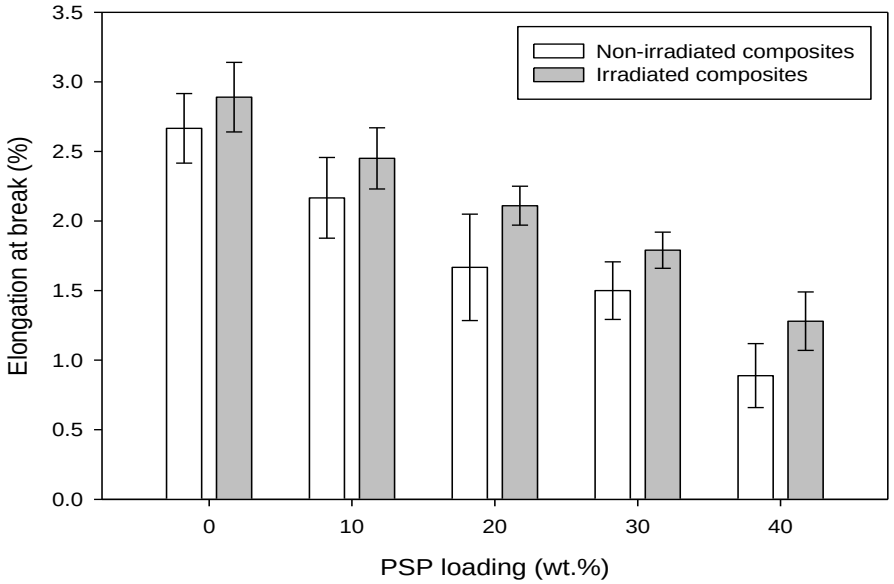

Fig. 6. Comparison of elongation at break after 6 months natural weathering

Figure 7 illustrates the tensile modulus of non-irradiated and irradiated composites after 6 months of natural weathering. The embrittlement of the composites is important in determining its tensile modulus (Younes *et al.* 2008).

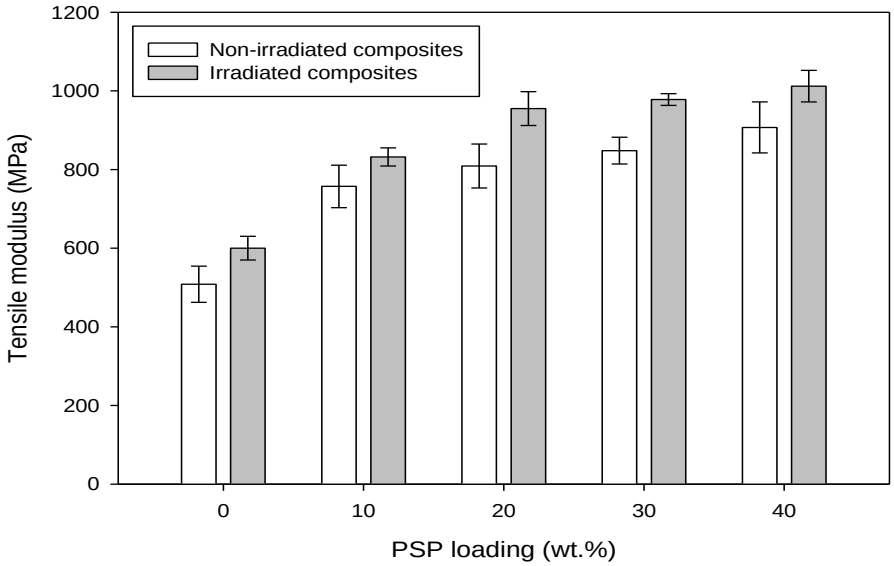

Fig. 7. Comparison of tensile modulus after 6 months natural weathering

The tensile modulus of both composites increased as PSP loading increased. The augmentation of tensile modulus was attributable to the creation of radical crosslinking for the duration of natural weathering exposure. The tensile modulus of irradiated composites was higher than non-irradiated composites. The crosslinked network generated by irradiation enhanced the interfacial adhesion between PSP and the RPP matrix. The flexibility and stiffness of irradiated composites was improved, leading to enhanced tensile modulus.

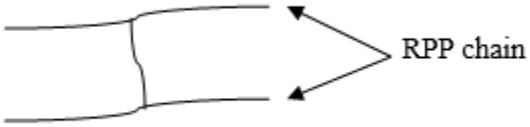

Fig. 8. Proposed crosslinking between propylene chains of RPP

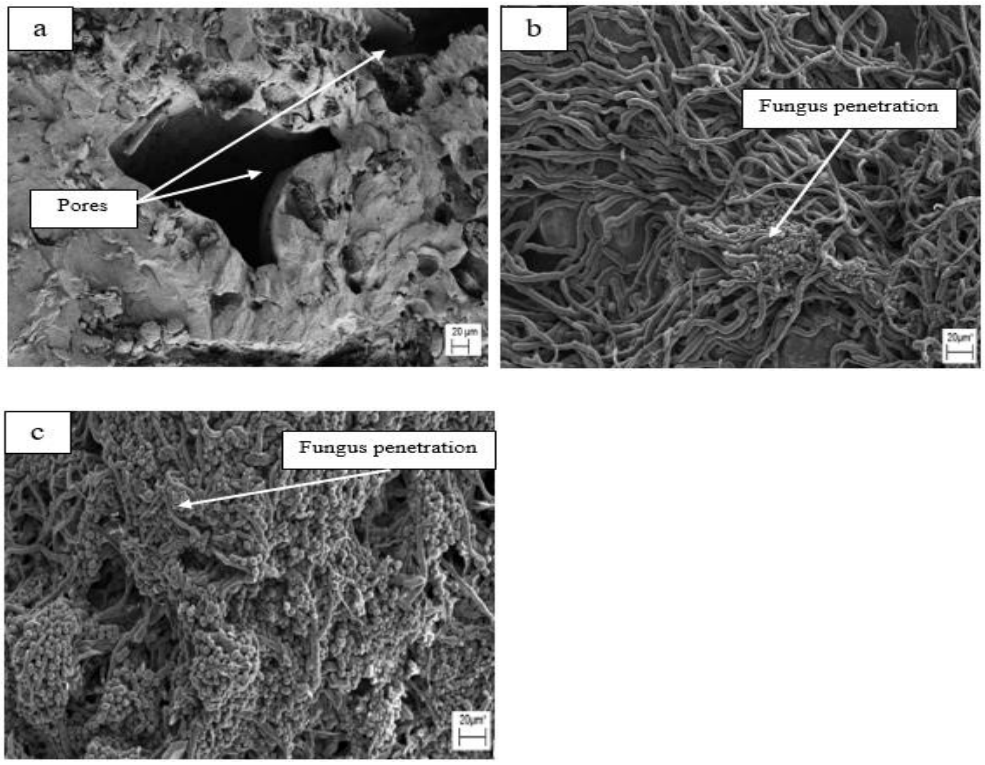

Fig. 9. SEM of non-irradiated RPP/PSP composites with (a) 10 wt.%, (b) 30 wt.%, and (c) 40 wt.% PSP loading after exposure to natural weathering for 6 months

Morphology of Weathered Samples

Figure 9 shows the surface morphology of the non-irradiated RPP/PSP composites after 6 months of natural weathering. In Figure 9(a), composites reinforced with low PSP loading (10 wt.%) exhibited a rough surface with a small amount of degradable substance (pores) deposited on the surface. The degradable components (likely PSP) were leached out to the surface upon weathering by rain and UV rays in sunlight.

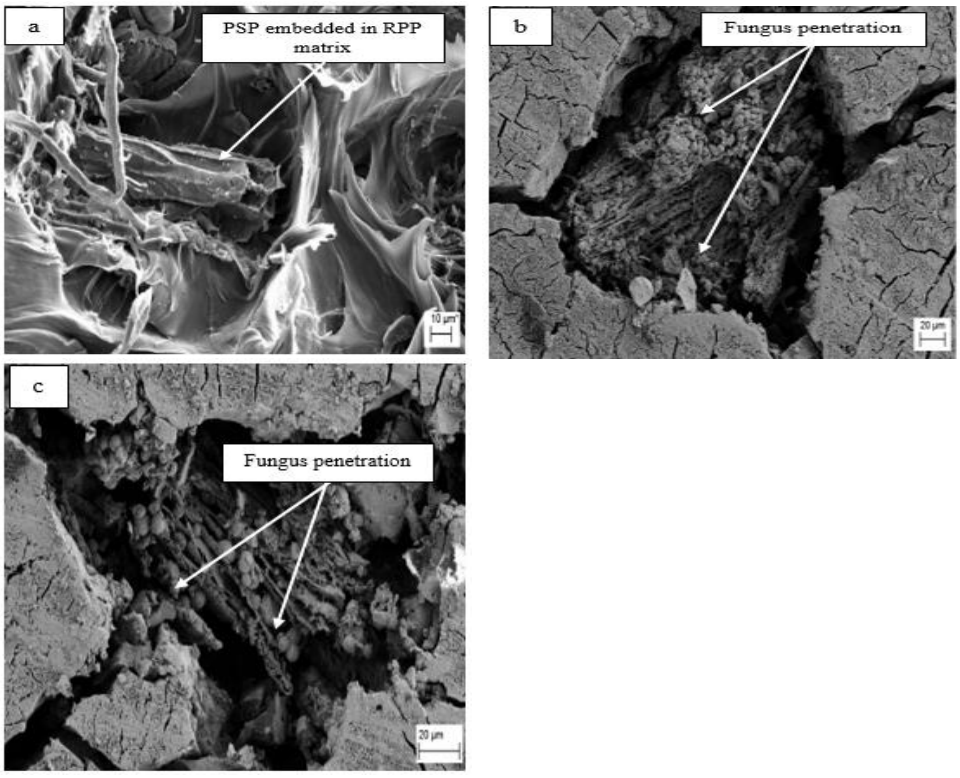

Fig. 10. SEM morphology of irradiated RPP/PSP composites with (a) 10 wt.% (b) 30 wt.% and (c) 40 wt. % of PSP loading after exposure to natural weathering for 6 months

The pore formation is explained by the occurrence of thermal contraction and material loss during natural weathering (Danjaji *et al*. 2002; Ahmad Thirmizir *et al*. 2010). With higher PSP loading (30 wt.% and 40 wt.%), the degradation of samples on the surface gradually penetrated the matrix. This result might be due to the formation of more surface cracks, which allow leaching out of the degradable components (PSP) and make the matrix more accessible to degradation (as shown in Fig. 9(b) and (c)). Indeed, PSP could undergo degradation upon EB irradiation; thus it would be easier to degrade during the weathering degradation test. Likewise, this structural damage allowed microorganisms to penetrate deeper into the composites and deteriorate the whole system. Consequently, the rate of biodegradation increased. This result was confirmed by the measured weight loss to be described in a later section.

Figure 10 displays the morphology of irradiated RPP/PSP composites after exposure to natural weathering for 6 months. Obviously, as can be seen from Fig. 10(a), PSP filler was embedded in RPP matrix, with less pores appearing on the surface. This showed that the homogeneity of filler dispersion and the filler-matrix interaction were improved due to the chain scission and crosslinking reaction, that were initiated by EB irradiation. Besides, after 6 months of exposure, the irradiated composites with 30 wt.% of

PSP loading had a rougher surface with different sizes and shapes of pores. This result was attributed to the cyclic expansion and contraction on the composites along with photo-degradation. The physical damage is initiated from the embrittlement of composites upon degradation. Thus, a larger surface area was formed for biotic and abiotic degradation. Biotic degradation was detected as the colonization of fungus on the sample surface (Fig. 10(b)). With greater PSP loading (40 wt.%), the degradation of composites at the surface penetrated into the matrix, as shown by the presence of fungus in Fig. 10(c). The formation of cracks and pores revealed that composites experienced the photo-degradation, thermal degradation, hydrolysis and microorganism's attack. Hence, weakened the filler-matrix interfacial adhesion and eventually, deteriorate the properties of the composite.

Carbonyl Indices

Figure 11 shows the FTIR spectra of irradiated composites before and after exposure to natural weathering. The spectra of all composites show similar trends except for small variations in the intensity in some absorption peaks and appearance of new peaks as a consequence of the weathering process. Upon EB irradiation, the main absorption peaks were observed at 3000-3600 cm^{-1}, 2915 cm^{-1}, 2858 cm^{-1}, and 1472 cm^{-1}, representing O-H stretching, C-H stretching, -CH_3 bending, and –CH_2- vibration, respectively. A peak at 1600-1800 cm^{-1} was assigned to stretching of the carbonyl group. After weathering, the intensity of OH groups and carbonyl groups increased slightly. These results can be explained on the basis of degradation factors, namely photo-oxidation, hydrolytic degradation, temperature, moisture or water absorption, and microbial attack. UV radiation breaks down the polymer chain and forms groups such as carbonyl and hydroxyl (Awang and Ismail 2009). In this case, the intensification of hydroxyl and carbonyl peaks confirmed that photo-degradation had occurred, resulting in changes in the chemical structure of the polymer (Ting *et al.* 2012). However, the value of carbonyl index for both non-irradiated and irradiated composites was relatively close after 6 months outdoor exposure, as shown in Fig. 12.

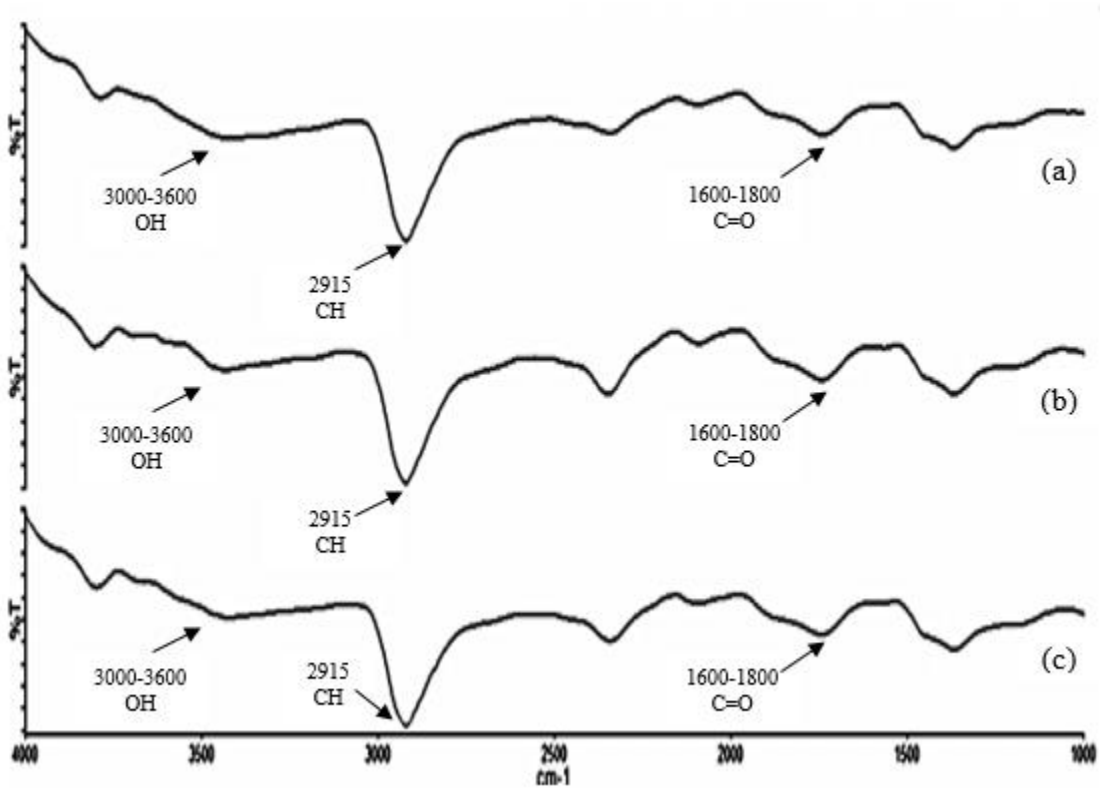

Fig. 11. FTIR spectra of irradiated RPP/PSP composites (a) unweathered with 10 wt.% PSP loading, (b) weathered with 10 wt.% PSP loading and (c) weathered with 40 wt.% PSP loading after 6 month natural weathering

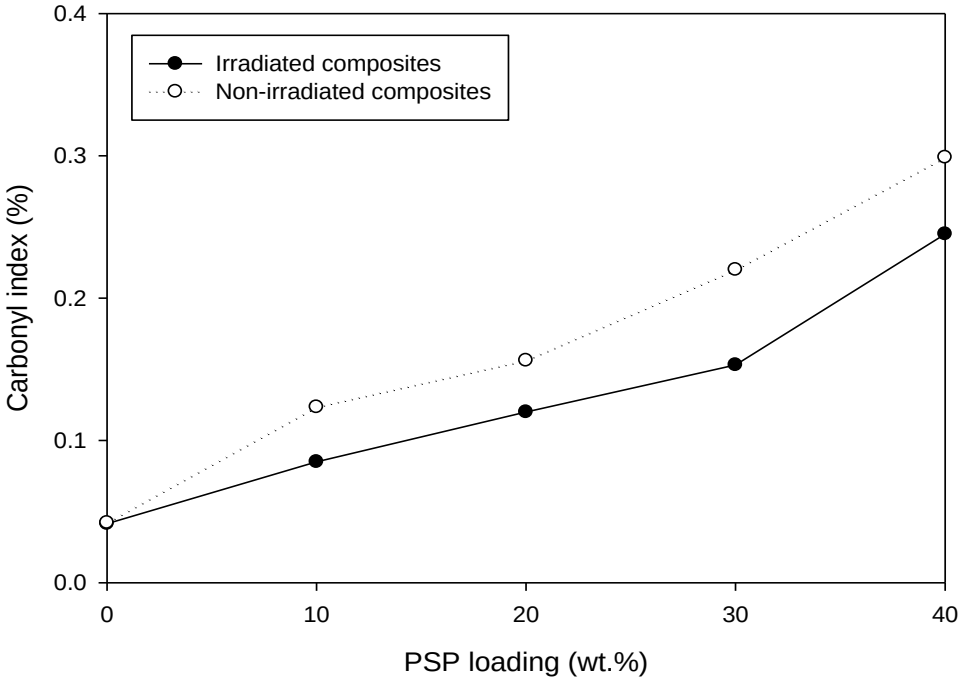

Fig. 12. CI for 10 wt.% PSP loading of non-irradiated and irradiated composites over a period of weathering for 6 months

Differential Scanning Calorimetry

Thermal characteristics are the main criteria for many practical applications of irradiated composites. Figures 13 and 14 demonstrate the representative melting and cooling curves of irradiated RPP/PSP composites before and after 6 months exposure to natural weathering. PSP loading of 10 wt.% was chosen to represent the thermal behavior of both composites because the heating and cooling trends for all composites were similar.

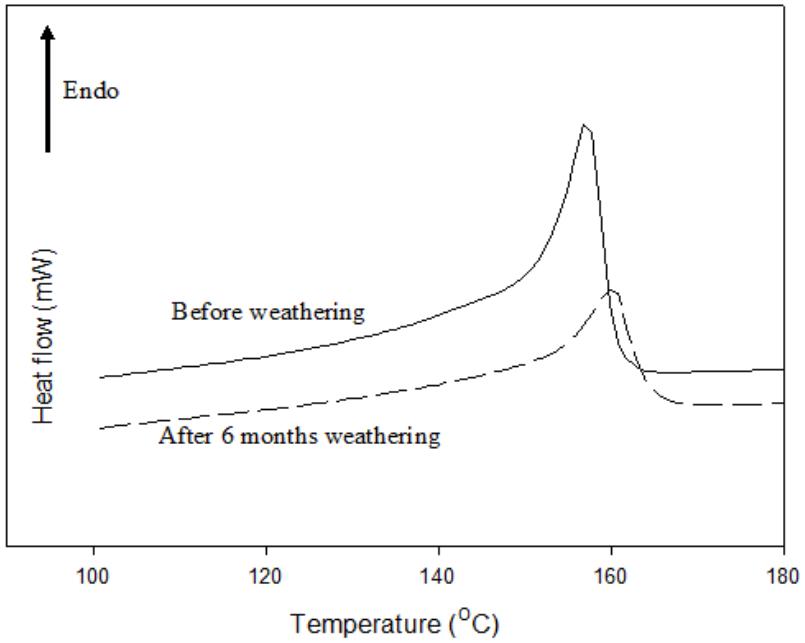

Fig. 13. DSC heating thermogram of 10 wt.% PSP loading of irradiated RPP/PSP composites after 6 months exposure to natural weathering

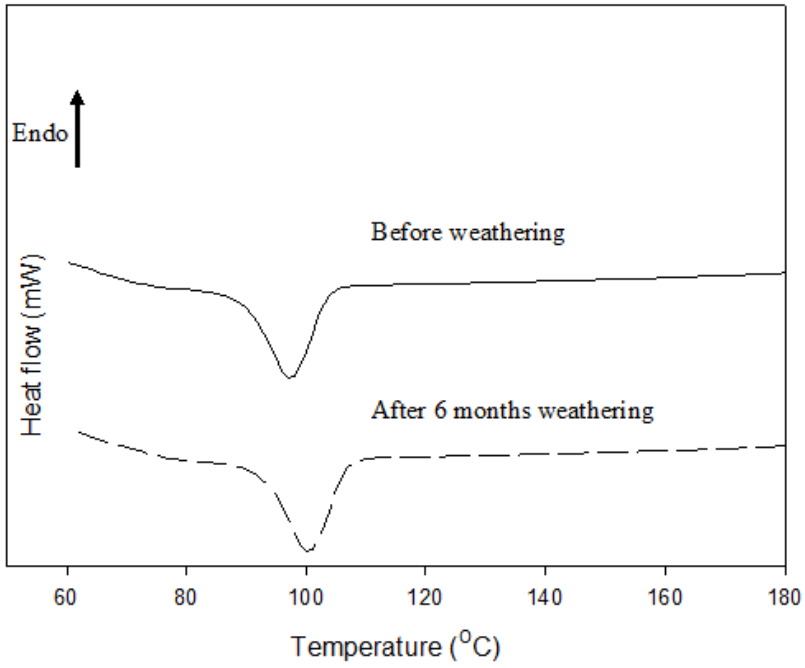

Fig. 14. DSC cooling thermogram of 10 wt.% PSP loading of irradiated RPP/PSP composites after 6 months exposure to natural weathering

Table 3 reports the melting temperature (T_m), crystallization temperature (T_c), enthalpy of fusion (ΔH_f), and degree of crystallinity (X_c). The trend of the heating thermogram (Fig. 13) and the melting point (Table 3) were similar. The results confirmed that there was no new crystalline phase formed upon degradation. However, the crystalline temperature and degree of crystallinity increased after exposure, which was attributed to the degradation of the amorphous phase. Khabbaz *et al.* (1999) reported that the amorphous phase in polymer experiences a higher hydrolysis rate, as well as oxidative and thermal degradation. Chain scission as a result of degradation also increases chain mobility, which accelerates crystallization in the amorphous phase. Consequently, the crystalline in the composites increased. Thus, the increased crystallinity of irradiated composites upon exposure only depended on the reduction of amorphous phase. PSP content also influenced the crystallinity transformation. As shown in Table 3, a higher PSP load resulted in higher crystallinity. As mentioned previously, the hydrophilic nature of PSP increases the leaching effect during degradation. The leaching effect generated crazes and pores on composite surfaces, which created more surface area and exposed the RPP matrix to microorganisms, heat, and UV. The UV degradation involves chain scission, which led to increases of the polymer chain mobility and crystallization. Thus, UV increased the degree of crystallinity while decreased the density of the entanglements in the amorphous phase (Stark and Matuana 2004). The crystallinity of irradiated composites was considerably lower than non-irradiated composites upon degradation. It was likely difficult for microorganisms to penetrate the crosslinked composites throughout exposure. Hence, the decrease of amorphous phase for irradiated composites was lower than in non-irradiated composites. Subsequently, the crystallinity of the irradiated composites was lower.

Table 3. DSC Data of Irradiated RPP/PSP Composites after 6 Months Exposure to Natural Weathering

Sample	T_m (°C)	T_c (°C)	ΔH_f (J/g)	Crystallinity (%)
RPP/10% PSP (non-irradiated)	165.84	110.59	83.87	45.02
RPP/30% PSP (non-irradiated)	163.72	111.21	78.43	54.13
RPP/40% PSP (non-irradiated)	160.01	111.74	72.45	58.33
RPP/10% PSP (irradiated)	158.71	108.46	54.25	29.12
RPP/30% PSP (irradiated)	148.15	109.00	44.34	30.60
RPP/40% PSP (irradiated)	145.08	111.05	42.03	33.84

Table 4. Weight Loss of Non-Irradiated and Irradiated RPP/PSP Composites

Sample	Weight Loss (%)	
	Non-irradiated	Irradiated
RPP	0.84	0.97
RPP/10% PSP	1.56	1.18
RPP/20% PSP	2.96	1.27
RPP/30% PSP	6.52	3.99
RPP/40% PSP	9.24	4.93

Weight Loss

The gravimetric analysis of the composites after exposure to natural weathering was achieved by measuring the sample weight loss. The weight loss of the degraded composites principally quantifies the loss of the hydrophilic materials. Table 4 displays the

weight loss of non-irradiated and irradiated RPP/PSP composites after 6 months exposure to natural weathering. The weight loss increased as PSP loading increased, indicating that the hydrophilic content of PSP fillers was leached out by the external force of rain water during outdoor exposure. Additionally, the consumption of hydrophilic content by microorganisms contributed to the weight loss. The irradiated composites demonstrated lower weight loss than the non-irradiated composites. The potential cause was due to the creation of crosslinking network upon irradiation, which resisted the leaching out of the hydrophilic components from the irradiated composites.

CONCLUSIONS

1. The tensile strength and elongation at break of the irradiated RPP/PSP composites was higher than those of the non-irradiated RPP/PSP composites over 6 months of natural weathering. The retention of tensile strength and elongation at break for both composites decreased as the PSP loading increased.
2. The tensile modulus and retention of tensile modulus for both composites increased after the exposure.
3. The irradiated RPP/PSP composites were more resistant to weathering degradation than the non-irradiated RPP/PSP composites.
4. The carbonyl index for both composites increased after exposure. The non-irradiated composites showed a higher carbonyl index than the irradiated composites. The irradiated composites had lower crystallinity than non-irradiated composites.
5. The weight loss of the non-irradiated composites was higher than that of the irradiated composites after the degradation period.
6. The mechanical, thermal and retention to degradation properties of irradiated RPP/PSP composites were improved in comparison to the non-irradiated RPP/PSP composites.

ACKNOWLEDGMENTS

The authors acknowledge the financial support provided by Universiti Sains Malaysia Postdoctoral Fellow Scheme.

REFERENCES CITED

Aji, I. S., Zinudin, E. S., Khairul, M. Z., Abdan, K., and Sapuan, S. M. (2013). "Induced tensile properties with EB-crosslinking of hybridized kenaf/palf reinforced HDPE composite," *Pertanika Journals of Science and Technology* 21, 135-140.

Albano, C., Reyes, J., González, J., Ichazo, M., Poleo, R. and Davidson, E. (2001). "Mathematical analysis of the mechanical behavior of 60 co-irradiated polyolefin blends with and without woodflour," *Polymer Degradation and Stability* 73, 39-45. DOI: 10.1016/s0141-3910(01)00065-9

Alessi, S., Dispenza, C., Fuochi, P. G., Corda, U., Lavalle, M., and Spadaro, G. (2007).

"E-beam curing of epoxy-based blends in order to produce high-performance composites," *Radiation Physics and Chemistry* 76, 1308-1311. DOI:10.1016/j.radphyschem.2007.02.021

Ali, Z., Youssef, H. A. and Afify, T. (2008). "Structure-properties of electron beam irradiated and dicumyl peroxide cured low density polyethylene blends," *Polymer Composites* 29, 1119–1124. DOI: 10.1002/pc.20366

ASTM D638 (2014). "Standard test method for tensile properties of plastics," ASTM International, West Conshohocken, USA.

Awang, M. and Ismail, H. (2009). "Weatherability of polypropylene/waste tire dust blends: Effects of trans-polyoctylene rubber and dynamic vulcanization," *Journal of Vinyl and Additive Technology* 15, 29-38. DOI: 10.1002/vnl.20172

Balaji, A. B., Ratnam, C. T., Khalid, M. and Walvekar, R. (2017). "Effect of electron beam irradiation on thermal and crystallization behavior of PP/EPDM blend," *Radiation Physics and Chemistry* 141, 179-189. DOI: 10.1016/j.radphyschem.2017.07.001

Bee, S. T., Hassan, A., Ratnam, C. T., Tee, T. T., and Sin, L. T. (2012). "Effect of montmorillonite on the electron beam irradiation alumina trihydrate added polyethylene and ethylene vinyl acetate nanocomposite," *Polymer Composites* 33, 1883-1892. DOI: 10.1002/pc.22328

Berejka, A. J., Cleland, M. R., Galloway, R. A., and Gregoire, O. (2005). "X-ray curing of composite materials," *Nuclear Instruments And Methods In Physics Research B* 241**,** 847. DOI: 10.1016/j.nimb.2005.07.188

Cesarino, I., Araujo, P., Domingues Jr., A. P., and Mazzfera, P. (2012). "An overview of lignin metabolism and its effect on biomass recalcitrance," *Brazilian Journal of Botany* 35, 303-311. DOI : 10.1590/S0100-84042012000400003

Chattopadhyay, S. K., Khandal, R. K., Uppaluri, R., and Ghoshal, A. K. (2010). "Mechanical, thermal, and morphological properties of maleic anhydride-g-polypropylene compatibilized and chemically modified banana-fiber-reinforced polypropylene composites," *Journal of Applied Polymer Science* 117, 1731-1740. DOI: 10.1002/app.32065

Choi, H. Y., Han, S. O., and Lee, J. S. (2008). "Surface morphological, mechanical and thermal characterization of electron beam irradiated fibers," *Applied Surface Science* 255, 2466-2473. DOI: 10.1016/j.apsusc.2008.07.171

Corbiere-Nicollier, T., Gfeller Laban, B., Lundquist, L., Leterrier, Y., Manson, J.-A. E., and Jolliet, O. (2001). "Life cycle assessment of biofibres replacing glass fibres as reinforcement in plastics," *Resources, Conservation and Recycling* 33, 267-287. DOI: 10.1016/S0921-3449(01)00089-1

Czvikovszky, T. (1996). "Electron-beam processing of wood fiber reinforced polypropylene," *Radiation Physics and Chemistry* 47, 425-430. DOI: 10.1016/0969-806X(95)00131-G

Dispenza, C., Alessi, S., and Spadaro, G. (2008). "Carbon fiber composites cured by gamma-radiation-induced polymerization of an epoxy resin matrix," *Adv. Polym. Technol.* 27, 163-171. DOI: 10.1002/adv.20127

Fang, Z., Liu, K., Chen, F., Zhang, L., and Guo, Z. (2014). "Cationic surfactant-assisted microwave-NAOH pretreatment for enhancing enzymatic hydrolysis and fermentable sugar yield from peanut shells," *BioResources* 9, 1290-1302.

Gad, Y. H. (2009). "Improving the properties of poly(ethylene-co-vinyl acetate)/clay composite by using electron beam irradiation," *Nuclear Instruments and Methods in*

Physics Research B 267, 3528-3534. DOI: 10.1016/j.nimb.2009.08.010

Gupta, A. P., Kumar, V., Sharma, M., and Shukla, S. K. (2009). "Physicochemical studies on interaction behaviour of potato starch filled low density polyethylene grafted maleic anhydride and low density polyethylene biodegradable composite sheets," *Polymer Plastic Technology and Engineering* 48, 587-594.

Henniges, U., Hasani, M., Potthast, A., Westman, G., and Rosenau, T. (2013). "Electron beam irradiation of cellulosic materials - Opportunities and limitations," *Materials* 6, 1584-1598. DOI: 10.3390/ma6051584

Ishak Ahmad, Chong Ee Lane, Dahlan H. M., and Abdullah, I. (2012). "Electron-beam-irradiated rice husk powder as reinforcing filler in natural rubber/high-density polyethylene (NR/HDPE) composites," *Composites: Part B* 43, 3069-3075. DOI: 10.1016/j.compositesb.2012.04.071

Ismail, H., Galpaya, D., and Ahmad, Z. (2010). "Electron beam irradiation of blends of polypropylene with recycled acrylonitrile butadiene rubber," *Journal of Vinyl Additives and Technology* 16, 141-146. DOI: 10.1002/vnl.20203

ISO 877.2 (2009). "Plastics-Methods of exposure to solar radiation-Part 2: Direct weathering and exposure behind glass," International Organization for Standardization, Geneva, Switzerland.

Khabbaz, F., Albertsson, A. C., and Karlsson, S. (1999). "Chemical and morphological changes of environmentally degradable polyethylene films exposed to thermo-oxidation," *Polymer Degradation and Stability* 63, 127-138. DOI: 10.1016/s0141-3910(98)00082-2

Khan, F., Ahmad, S. R. , and Kronfli, E. (1999). "Stability of jute fibres on exposure to ionising radiation," *Polymer Degradation and Stability* 63, 79-84. DOI: 10.1016/S0141-3910(98)00064-0

Mizera, A., Manas, M., Holik, Z., Manas, D., Stanek, M., Cerny, J., Bednarik, M., and Ovsik, M. (2012). "Properties of selected polymers after radiation crosslinking," *International Journal of Mathematics and Computers in Simulation* 6, 592-599.

Murray, K. A., Kennedy, J. E., Mcevoy, B., Vrain, O., Ryan, D., Cowman, R. and Higginbotham, C. L. (2013). "The effect of high energy electron beam irradiation in air on accelerated aging and on the structure property relationships of low density polyethylene," *Nuclear Instruments and Methods in Physics Research B* 297, 64-74. DOI: 10.1016/j.nimb.2012.12.001

Nordin, R., and Ismail, H. (2013). "Electron beam treatment for enhancing the compatibility, thermal and tensile properties of LLDPE/PVA blends: Part I, Effect of irradiation doses," *International Journal of Engineering Research and Application* 3, 1820-1825.

Obasi, H. C. (2015). "Peanut husk filled polyethylene composites: Effects of filler content and compatibilizer on properties," *Journal of Polymers and the Environment* 2015, 1-9. DOI: 10.1155/2015/189289

Raju, G. U., Kumarappa, S., and Gaitonde, V. N. (2012). "Mechanical and physical characterization of agricultural waste reinforced polymer composites," *Journal of Materials and Environmental Science* 3, 907-916.

Sabet, M., Hassan, A., and Ratnam, C. T. (2012). "Mechanical, electrical and thermal properties of irradiated low density polyethylene by electron beam," *Polymer Bulletin* 68, 2323-2339. DOI: 10.1007/s00289-012-0741-y

Salmah, H., Romisuhani, A., and Akmal, H. (2011). "Properties of low-density polyethylene/palm kernel shell composites: Effect of polyethylene co-acrylic acid,"

Journal of Thermoplastic Composite Materials 26, 3-15. DOI: 10.1177/0892705711417028

Sam, S. T., Ismail, H., and Ahmad, Z. (2012a). "Study on electron beam irradiated linear low density polyethylene/soya powder blends under outdoor exposure," *Journal of Vinyl Additives and Technology* 18, 241-249. DOI: 10.1002/vnl./20327

Sam, S. T., Ismail, H., Ahmad, Z., and Ratnam, C. T. (2012b). "Effect of electron beam irradiation on the properties of epoxidized natural rubber (ENR 50) compatibilized linear low density polyethylene/soya powder blends," *Journal of Applied Polymer Science* 124, 5220-5228. DOI: 10.1002/app.34136

Santiagoo, R., Affandi, R. D., Noraishah, S., Ismail H., and Hussin, K. (2016). "The compatibilizing effect of polypropylene maleic anhydride (PPMAH) on polypropylene (PP)/acrylonitrile butadiene rubber (NBR)/palm kernel shell (PKS) composites," *ARPN Journal of Engineering and Applied Sciences* 11, 1666-1672.

Shubhra, Q. T. H., Alam, A., and Quaiyyum, M. A. (2011). "Mechanical properties of polypropylene composites: A review," *Journal of Thermoplastic Composite Materials* 26, 362-391. DOI: 10.1177/0892705711428659

Stark, N. M., and Matuana, L. M. (2004). "Surface chemistry changes of weathered HDPE/wood flour composites studied by XPS and FTIR spectroscopy," *Polymer Degradation and Stability* 86, 1-9. DOI: 10.1016/j.polymdegradstab.2003.11.002

Ting, S. S., Ismail, H., and Ahmad, Z. (2012). "Environmental weathering of (linear low-density polyethylene)/(soya powder) blends compatibilized with polyethylene-grafted maleic anhydride," *Journal of Vinyl and Additive Technology* 18, 57-64. DOI: 10.1002/vnl.20292

Wilson, K., Yang, H., Seo, C. W., and Marshall, W. E. (2006). "Select metal adsorption by activated carbon made from peanut shells," *Bioresource Technology* 97, 2266-2270. DOI: 10.1016/j.biortech.2005.10.043

Younes, M. M., Abdel-Rahman, H. A., Orabi, W., and Ismail, M. R. (2008). "Effect of electron beam irradiation on physical-mechanical properties of wood flour-polyethylene composites," *Polymer Composites* 29, 768-772. DOI 10.1002/pc.20491

Youssef, H. A., Ismail, M. R., Ali, M. A. M., and Zahran, A. H. (2009). "Studies of sugarcane baggase fiber-thermoplastic composites," *Journal of Elastomers and Plastics* 41, 245-262.

Zhai, M., Yoshii, F., and Kume, T. (2003). "Radiation modification of starch-based plastic sheets," *Carbohydrate Polymers* 52, 311-317. DOI: 10.1016/S0144-8617(02)00292-8

Zheng, W., Phoungthong, K., Lu, F., Shao, L. M., and He, P. J. (2013). "Evaluation of a classification method for biodegradable solid wastes using anaerobic degradation parameters," *Waste Management* 33, 2632-2640. DOI: 10.1016/j.wasman.2013.08.015

Article submitted: September 10, 2017; Peer review completed: November 5, 2017; Revised version received: November 16, 2017; Accepted: November 17, 2017; Published: November 22, 2017.
DOI: 10.15376/biores.13.1.487-505